Electrons and holes in InSb under crossed magnetic and stress fields. I. Theory

H. -R. Trebin

*Institut für Theoretische und Angewandte Physik, Universität Stuttgart,
D-7000 Stuttgart 80, West Germany*

B. Wolfstädter*

Physikalisches Institut, Universität Würzburg, D-8700 Würzburg, West Germany

H. Pascher

Physikalisches Institut, Universität Bayreuth, D-8580 Bayreuth, West Germany

H. Häfele

Physikalisches Institut, Universität Würzburg, D-8700 Würzburg, West Germany

In a series of four papers magnetooptical transitions are presented for InSb crystals, which are subjected to uniaxial stress perpendicular to the magnetic field. Here, in the first paper, we establish an 8×8 k·p Hamiltonian matrix for stress $T \| [100]$ and field $B \| [001]$ and diagonalize it exactly. The dependence of valence and conduction states on stress and longitudinal momentum is discussed and compared with the geometry of parallel fields $T \| B \| [001]$. Characteristic features are extracted for inter- and intraband transitions. Under crossed fields, the levels are separated much stronger with stress, yielding more insight than in the parallel configuration.

I. INTRODUCTION

The electronic energy bands of zinc-blende structure semiconductors exhibit significant deviations from the simple isotropic and parabolic shape close to the gap. In both conduction[1] and valence bands[2] one finds strong terms of cubic and quartic order in k and warping. Uniaxial stress induces k-linear terms which shift the band extrema to nonzero wave vectors.[3] For the valence bands k-linear terms exist already in the unstressed state.[4] The band anomalies can be detected in Shubnikov–de Haas oscillations,[3] in spin-depolarization measurements,[5] or in far-infrared and Raman scattering experiments on doped semiconductors.[6]

Under the influence of a magnetic field, the spin-degenerate conduction bands form two Landau ladders, which, due to the nonparabolicities, are spaced irregularly. The differences in the spacings show up in splittings of the harmonic transition lines. The cyclotron mass and g factor are field dependent.[7] Higher harmonic and spin-flip transitions become allowed.[8]

The uppermost valence band is fourfold degenerate at $k=0$. In a magnetic field, the four bands turn into four entangled Landau ladders with strongly varying separations of the rungs. Magnetooptical transitions can only be identified reliably if by application of uniaxial stress the band degeneracy is lifted and the ladders are pulled apart.

Such a program was first pursued by Hensel and Suzuki[9] in the investigation of the valence bands of Ge. For most of their experiments, stress was applied parallel to the magnetic field along the crystal [001], [111], and [110] directions, and microwave absorption was regis-

tered. The spectra were calculated from an effective-mass Hamiltonian which was formed in the space of the four degenerate valence-band functions of symmetry Γ_8^+. Given the geometry of the experiments and the diamond lattice structure of Ge, the symmetry groups of this Hamiltonian are C_4 (consisting of rotations about the direction of the magnetic field by multiples of $2\pi/4$), C_3, and C_2, respectively. The symmetries permit a simple labeling scheme for the magnetic states and simplify the numerical calculations.

Similar experiments were performed soon afterwards by Ranvaud et al.[10] Since Ranvaud used far-infrared radiation, higher magnetic fields had to be applied than were necessary in the microwave experiments of Hensel and Suzuki.[9] The strong fields (up to 8 T) and the small gap of InSb required that in the theoretical evaluation the number of basis states for the k·p Hamiltonian be enlarged. The basis finally consisted of the four Γ_8 valence states, the two Γ_7 split-off band states, and the two Γ_6 conduction states.[11] The zinc-blende lattice is lacking the inversion symmetry of the diamond lattice. Inversion-asymmetry terms reduce the symmetry of the k·p Hamiltonian from C_4 to C_2, if stress and magnetic field are applied parallel to the [001] direction.

Ranvaud's intraband quantum cyclotron-resonance spectra provided deep insight into the energy structure of holes in InSb. The set of band parameters, which was derived in the fit of field and pressure dependence of the spectral lines, disagrees, however, with data used in interpreting interband absorption spectra and intra-conduction-band measurements (see, for example, Ref. 12). In these measurements, no advantage was taken of the band resolving power which uniaxial stress offers.

To enhance the knowledge of the magnetic band struc-

ture, we present a series of magnetooptical experiments on uniaxially stressed InSb in four successive articles. In all cases the magnetic field is applied along the [001] direction. Contrary to previous investigations, the direction of the uniaxial stress is perpendicular to the magnetic field, namely along [100]. For the k·p theory, the geometry of crossed fields is not inferior to the geometry of parallel fields, since the symmetry group of the Hamiltonian remains the two element group C_2. From the experimental point of view, the geometry is easier to realize and yields an even higher resolution of the bands. In the group C_2 all symmetry breaking effects are taken into account: the tetrahedral crystal point group, magnetic and strain field, and longitudinal momentum k_B.

In the present paper we establish an effective-mass Hamiltonian that describes the band-edge states in a magnetic field along the [001] direction and in a stress field parallel to the [100] direction. We also add terms to the Hamiltonian, which take into account the k·p, magnetic, and strain interaction of the eight basis states with the spin-orbit split Γ_7^c and Γ_8^c conduction states. These states are separated by 3 eV from the gap. The Hamiltonian is diagonalized, and the spectra are discussed. We used the band parameters from the work of Ranvaud et al.,[10] supplemented by data from Ref. 8.

In the second paper of this series[13] we report the observation of optically pumped recombination radiation. Interband transitions were detected which reveal some of the valence-band fine structure.

The third paper of this series[14] describes magnetoreflection spectra under varying stress loads.

The final paper of this series[15] is concerned with hole Raman scattering in the valence bands of InSb. From the data features are extracted that characterize the depen-

dence of the energies on the longitudinal momentum k_B.

The theory can identify all the observed spectral lines. Although in several cases the exact line positions disagree, the stress dependence and the oscillator strengths of the transitions are unique. However, we did not attempt to derive another set of band parameters, because the amount of experimental data still seems to be insufficient.

II. GENERAL FORM OF THE EFFECTIVE-MASS HAMILTONIAN

The Hamiltonian, on which we base the following calculations, has been established in Ref. 11. In this section we briefly repeat its construction principles and present additional terms, which arise from the interaction of the gap states with higher conduction states.

The 8×8 Hamiltonian matrix falls into nine blocks:

$$H = \begin{bmatrix} H^{cc} & H^{cv} & H^{cs} \\ H^{vc} & H^{vv} & H^{vs} \\ H^{sc} & H^{sv} & H^{ss} \end{bmatrix} . \tag{1}$$

H^{cc} and H^{ss} are 2×2 intraband matrices for the Γ_6 conduction and Γ_7 spin-orbit split valence states, and H^{vv} is the 4×4 intraband matrix of the Γ_8 valence states closest to the band edge. H^{cv}, H^{cs}, and H^{vs} are interband matrices, forming 2×4, 2×2, and 4×2 blocks, respectively, and H^{vc}, H^{sc}, and H^{sv} are their Hermitian conjugates.

The elements of each block consist of polynomials in the components of the wave vector k, the magnetic induction B, and the strain tensor $\tilde{\epsilon}$. Each block has been expanded into products of basis matrices (spanning the respective space of $n \times m$ matrices) and basis polynomials (in the components of k, B, and $\tilde{\epsilon}$).

TABLE I. Invariant expansion of the blocks $H^{\alpha\beta}$ of the Hamiltonian matrix. Compared to Table IV of Ref. 11 the notation B instead of H is used and interaction terms with the p-antibonding bands have been added. c.p. denotes cyclic permutation of the preceding term and $\text{tr}\tilde{\epsilon} = \epsilon_{xx} + \epsilon_{yy} + \epsilon_{zz}$.

$$H^{cc} = E_g + \frac{\hbar^2 k^2}{2m}(1+2F) - (g_s - 4N_1)\frac{e\hbar}{4mc}(\sigma \cdot B) + C_1 \text{tr}\tilde{\epsilon}$$

$$H^{vv} = H_k^{vv} + H_\epsilon^{vv} + H_{kl}^{vv} + H_{\epsilon k}^{vv}$$

$$H_k^{vv} = -(\hbar^2/m)\{\tfrac{1}{2}\gamma_1 k^2 - \gamma_2[(J_x^2 - \tfrac{1}{3}J^2)k_x^2 + \text{c.p.}] - 2\gamma_3[\tfrac{1}{2}(J_x J_y + J_y J_x)\tfrac{1}{2}(k_x k_y + k_y k_x) + \text{c.p.}]\}$$
$$\quad - (e\hbar/mc)[(\kappa J_x + q J_x^3)B_x + \text{c.p.}]$$

$$H_\epsilon^{vv} = D_d \text{tr}\tilde{\epsilon} + \tfrac{2}{3}D_u[(J_x^2 - \tfrac{1}{3}J^2)\epsilon_{xx} + \text{c.p}] + \tfrac{2}{3}D_u'[2\tfrac{1}{2}(J_x J_y + J_y J_x)\epsilon_{xy} + \text{c.p.}]$$

$$H_{kl}^{vv} = (2C/\sqrt{3})\{\tfrac{1}{2}[J_x(J_y^2 - J_z^2) + (J_y^2 - J_z^2)J_x]k_x + \text{c.p.}\}$$

$$H_{\epsilon k}^{vv} = [C_4(\epsilon_{yy} - \epsilon_{zz})k_x + C_5'(\epsilon_{xy}k_y - \epsilon_{xz}k_z)]J_x + \text{c.p.}$$

$$H^{ss} = -[\Lambda + (\hbar^2/2m)\gamma_1 k^2] - 2\kappa(e\hbar/2mc)(\sigma \cdot B) + D_d \text{tr}\tilde{\epsilon}$$

$$H^{cv} = \sqrt{3}\{P(k_x T_x + \text{c.p.}) + iB[T_x \tfrac{1}{2}(k_y k_z + k_z k_y) + \text{c.p.}] + iC_2(T_x \epsilon_{yz} + \text{c.p.})\}$$
$$\quad + \frac{3\hbar^2}{m}\left[\frac{3}{2}\right]^{1/2} N_2[(k_z^2 - \tfrac{1}{3}k^2)(T_{xx} - T_{yy}) - (k_x^2 - k_y^2)T_{zz}] + \frac{\sqrt{6}}{i}N_3\frac{e\hbar}{mc}(B_x T_{yz} + \text{c.p.})$$

$$H^{cs} = -(1/\sqrt{3})\{P(\mathbf{k} \cdot \rho) + iB[\rho_x \tfrac{1}{2}(k_y k_z + k_z k_y) + \text{c.p.}] + iC_2(\rho_x \epsilon_{yz} + \text{c.p.})\}$$

$$H^{vs} = H_k^{vs} + H_\epsilon^{vs} + H_{\epsilon k}^{vs}$$

$$H_k^{vs} = -(\hbar^2/m)\{-3\gamma_2(U_{xx}k_x^2 + \text{c.p.}) - 6\gamma_3[U_{xy}\tfrac{1}{2}(k_x k_y + k_y k_x) + \text{c.p.}]\} - (e\hbar/mc)\tfrac{3}{2}\kappa(U_x B_x + \text{c.p.})$$

$$H_\epsilon^{vs} = 2D_u(U_{xx}\epsilon_{xx} + \text{c.p.}) + 2D_u'(2U_{xy}\epsilon_{xy} + \text{c.p.})$$

$$H_{\epsilon k}^{vs} = \tfrac{3}{2}[C_4(\epsilon_{yy} - \epsilon_{zz})k_x + C_5'(\epsilon_{xy}k_y - \epsilon_{xz}k_z)]U_x + \text{c.p.}$$

It is known how the polynomials transform under point group operations, since their variables are components of Cartesian tensors. The transformation properties of the basis matrices are determined by the behavior of the corresponding wave functions under the operations of the crystal point group.[16]

In the expansion special bases both in the space of matrices and in the space of polynomials have been used which transform according to irreducible representations of the crystal point group T_d. This choice immediately yields invariants of the group T_d and of the time reversal operation, out of which the blocks must be composed. The symmetry adapted matrix and polynomial bases are presented in Ref. 11. [There is a misprint in Table I of Ref. 11: the sign of component $(T_{xx})_{21}$ must be reversed such that $(T_{xx})_{21} = -\sqrt{3/2}$.]

The factors weighing the invariant terms are material constants. They can be determined by a fit to experimental data, but also by comparison with a perturbation matrix. This matrix arises if the eight band-edge states are considered as quasidegenerate, being mixed by $\mathbf{k} \cdot \mathbf{p}$, magnetic, and strain interactions.

In Ref. 11, which aimed at computing valence-band levels, several less important invariants have been omitted in H^{cc} and H^{cv}. However, as stated by Ogg,[17] Hermann and Weisbuch,[18] Weiler et al.,[8] and Rössler,[1] interaction terms with the higher conduction states Γ_8^c and Γ_7^c (p-antibonding states) appreciably influence the energy of the lowest conduction electrons. Since we are going to probe magnetic states also in the conduction bands, the following terms, which have been elaborated, for instance in Ref. 8, were added to the Hamiltonian of Trebin et al.:[11] (i) The bare conduction-band g factor,

$g_s = -2.0023$, is modified to $g = g_s - 4N_1$. The parameter N_1 has been carefully studied recently by Chen et al.[7] and Cardona.[19] (ii) Two new invariants appear in H^{cv}, weighed by factors N_2 and N_3.

The expansion of the blocks $H^{\alpha\beta}$ is presented in Table I. It corresponds to Table IV of Ref. 11, where some minor misprints have been corrected and the interaction terms with the p-antibonding bands have been inserted. We replaced the correction A' of the bare conduction-band mass by the more frequently used notation $F = mA'/\hbar^2$.

III. SPECIAL FORM OF THE EFFECTIVE-MASS HAMILTONIAN

In the effective-mass Hamiltonian we now specialize the magnetic induction to $\mathbf{B} = (0,0,B)$, pointing along the [001] direction, and the strain tensor to

$$\epsilon_{yy} = \epsilon_{zz} = s_{12}T ,$$

$$\epsilon_{xx} = s_{11}T ,$$ (2)

$$\epsilon_{xy} = \epsilon_{yz} = \epsilon_{zx} = 0 ,$$

arising from uniaxial stress along the [100] direction. The stress is denoted by T and s_{ij} are the cubic elastic compliance constants.

Introducing dimensionless coefficients, oscillator operators, and basis matrices in cylinder coordinates as in Ref. 11, we obtain the effective-mass Hamiltonian of Table II. The blocks $H^{\alpha\beta}$ are expressed in units of the cyclotron energy $\hbar\omega_c$ and are designated $D_{\alpha\beta}$. They are divided into contributions $D_{\alpha\beta}^a$, $D_{\alpha\beta}^c$, and $D_{\alpha\beta}^t$. The operators $D_{\alpha\beta}^a$ have cylinder symmetry C_∞, and the operators

TABLE II. Blocks of the Hamiltonian matrix in magnetic units and cylinder coordinates for $B\|[001]$, $T\|[100]$. For the notation see Ref. 11. The terms which have changed in comparison to Table VI of Ref. 11 are set in curly brackets.

$$D_{cc}^a = e_g + \{(1+F/2)S - \tfrac{1}{4}(g_s^0 - 4N_1)\sigma_3\} + x_c$$

$$D_{vv}^a = -\gamma_1 S - \gamma_2 S_0 + 2\gamma_3 S_1 + \tfrac{1}{2}(\gamma_2 + \gamma_3)S_2 - \kappa J_3 - qJ_3^3 + \{\tfrac{3}{2}c_4\zeta J_3 - \tfrac{3}{4}c_4(a^\dagger J_- + aJ_+)\} + x_d - \{\tfrac{1}{2}x_u(J_3^2 - \tfrac{5}{4})\}$$

$$D_{ss}^a = -\lambda - \gamma_1 S - \kappa\sigma_3 + x_d$$

$$D_{cv}^a = \sqrt{3}p_s(a^\dagger T_- + aT_+ + \zeta T_3)$$

$$D_{cs}^a = -(1/\sqrt{3})p_s(a^\dagger \rho_- + a\rho_+ + \zeta \rho_3)$$

$$D_{vs}^a = -3\gamma_2\tilde{S}_0 + 6\gamma_3\tilde{S}_1 + \tfrac{3}{2}(\gamma_2 + \gamma_3)\tilde{S}_2 - \tfrac{3}{2}\kappa U_3 + \{\tfrac{9}{4}c_4\zeta U_3 - \tfrac{9}{8}c_4(a^\dagger U_- + aU_+) - \tfrac{3}{2}x_u U_{33}\}$$

$$D_{vv}^c = \tfrac{1}{2}(\gamma_2 - \gamma_3)(J_+^2 a^{\dagger 2} + J_-^2 a^2)$$

$$D_{vs}^c = \tfrac{3}{2}(\gamma_2 - \gamma_3)(U_{++}a^{\dagger 2} + U_{--}a^2)$$

$$D_{vv}^t = -(c/\sqrt{3})[a^\dagger(J_-^3 - \tfrac{11}{4}J_+ + 3J_3 J_+ J_3 + J_+ J_- J_+) + a(J_+^3 - \tfrac{11}{4}J_- + 3J_3 J_- J_3 + J_- J_+ J_-)$$
$$\quad - 2\zeta(J_+ J_3 J_+ + J_- J_3 J_-)] + \{\tfrac{3}{4}c_4(a^\dagger J_+ - aJ_-) + \tfrac{1}{2}x_u(J_+^2 + J_-^2)\}$$

$$D_{cv}^t = \sqrt{3}b[\zeta(a^\dagger T_+ - aT_-) + \tfrac{1}{2}(a^{\dagger 2} - a^2)T_3]$$
$$\quad + \{-3\sqrt{3/2}N_2[\tfrac{2}{3}(a^\dagger a + \tfrac{1}{2} - \zeta^2)(T_{++} + T_{--}) + (a^{\dagger 2} + a^2)T_{33}]\} - \{\tfrac{1}{2}\sqrt{6}N_3(T_{++} - T_{--})\}$$

$$D_{cs}^t = -(1/\sqrt{3})b[\zeta(a^\dagger \rho_+ - a\rho_-) + \tfrac{1}{2}(a^{\dagger 2} - a^2)\rho_3]$$

$$D_{vs}^t = \{\tfrac{9}{8}c_4(a^\dagger U_+ + aU_-) + \tfrac{3}{2}x_u(U_{++} + U_{--})\}$$

$$S = a^\dagger a + \tfrac{1}{2} + \tfrac{1}{2}\zeta^2$$

$$S_0 = (J_3^2 - \tfrac{5}{4})(a^\dagger a + \tfrac{1}{2} - \zeta^2) \qquad\qquad \tilde{S}_0 = U_{33}(a^\dagger a + \tfrac{1}{2} - \zeta^2)$$

$$S_1 = \tfrac{1}{2}(J_3 J_+ + J_+ J_3)\xi a + \tfrac{1}{2}(J_3 J_- + J_- J_3)\xi a^\dagger \qquad \tilde{S}_1 = U_{3+}\zeta a + U_{3-}\zeta a^\dagger$$

$$S_2 = J_+^2 a^2 + J_-^2 a^{\dagger 2} \qquad\qquad\qquad \tilde{S}_2 = U_{++}a^2 + U_{--}a^{\dagger 2}$$

$D^c_{\alpha\beta}$ have symmetry C_4 due to cubic terms of the crystal field. Finally, the parts $D^t_{\alpha\beta}$ are of symmetry C_2 due to tetrahedral crystal-field terms and stress terms. In Ref. 11, the division of the Hamiltonian matrix was refined still more, leading to six stages of symmetry breaking, which have been denoted M_0–M_5. Stage M_5 of lowest symmetry—C_2—was due to tetrahedral crystal-field terms of finite longitudinal momentum k_B. In the present geometry of crossed fields also $k_B = 0$ terms contribute to stage M_5, viz., those which originate from the transversal stress.

IV. EIGENSTATES

The magnetic eigenstates are expanded into basis states $|\zeta;n\alpha M\rangle$. These are products of plane waves of wave vector ζ along the magnetic field; of pure oscillator states carrying n quanta; and of spin states in the band $\alpha \in \{c,v,s\}$ carrying magnetic quantum number M.

The division of the Hamiltonian matrix into parts of descending symmetry leads to a series of labels for each eigenstate, e.g., $N_n K^\tau Q P$ for $\mathbf{B}\|[001]$. The only good quantum number is $P \in \{0,1\}$, denoting an irreducible representation of the exact symmetry group C_2 of the Hamiltonian. The other labels are only approximate quantum numbers unless lower symmetry parts of the Hamiltonian vanish and thus raise the symmetry. For simplicity we frequently label the states by (n,M) or by a consecutive numbering $z\alpha$, $z = 1,2,3,\ldots$, $\alpha \in \{c,v,s\}$. A level scheme for zero stress and zero longitudinal momentum is presented in Fig. 1.

With the help of the symmetry labels selection rules are established for optical inter- and intraband transitions and qualitative conclusions can be drawn about their strength. For an exact identification of several transitions we calculated the transition matrix element $\langle f \mid u_s \mid i \rangle$ of the dimensionless velocity operator

$$u_s = (c/\hbar eB)^{1/2} m v_s .\qquad(3)$$

The final state is denoted by f, the initial state by i; $s \in \{x,y,z\}$ characterizes linear polarization, $s \in \{+,-\}$ circular polarization. The value of the matrix element is 1 for harmonic intraband transitions between pure oscillator states.

V. STRESS DEPENDENCE OF THE LANDAU LEVELS AT $k_B = 0$

Figures 2(a) and 2(b) show how the magnetic states close to the gap behave under stress parallel and perpendicular to the magnetic field. The material parameters are the same as in Ref. 11, and for the constants F, N_1, N_2, and N_3 we used the data of Weiler et al.:[8]

$$F = -3.4, \quad N_1 = -0.35 ,$$
$$N_2 = 0.23, \quad N_3 = 0.23 .\qquad(4)$$

The magnetic induction is held fixed at 2.0 T, the longitudinal momentum at $k_B = 0$. We have inverted the energy scale; hence the conduction states are situated at the bottom of the figures, the valence states at the top. All energies are referred to the lowest conduction state $1C = (0,\frac{1}{2})$, which appears as a flat band. For recombination radiation from this reference state, the diagram directly displays the stress dependence of the frequency.

At $k_B = 0$, the symmetry for $T\|\mathbf{B}\|[001]$ is S_4. The group is generated by a 90° rotation about the field direction, followed by the inversion operation. There are four irreducible representations, i.e., four noninteracting sets of Landau levels, labeled by $Q \in \{0,1,2,3\}$. Roughly speaking, each level interacts with the fourth one following.

For $T\perp\mathbf{B}$ the symmetry is lowered to C_2, even at $k_B = 0$, and two sets of levels exist, which are distinguished by the quantum number $P \in \{0,1\}$. Each level interacts with the second next one by stress terms of stage M_5. This fact explains the strong fanning of the energies.

For $T\|\mathbf{B}$, anticrossing effects become visible at 1980 cm^{-1}. They are related to the final state $7V = (1,-\frac{1}{2})$ of the "fundamental transition."[9] In Ge this state runs without interaction across the other lines, exactly parallel to the initial state $3V = (0,-\frac{1}{2})$. Owing to stress-induced

FIG. 1. Schematic representation of the zero stress Landau levels for $\mathbf{B}$ along the [001] direction and $k_B = 0$. A simplified notation is used and reference is made to the Pidgeon-Brown classification.
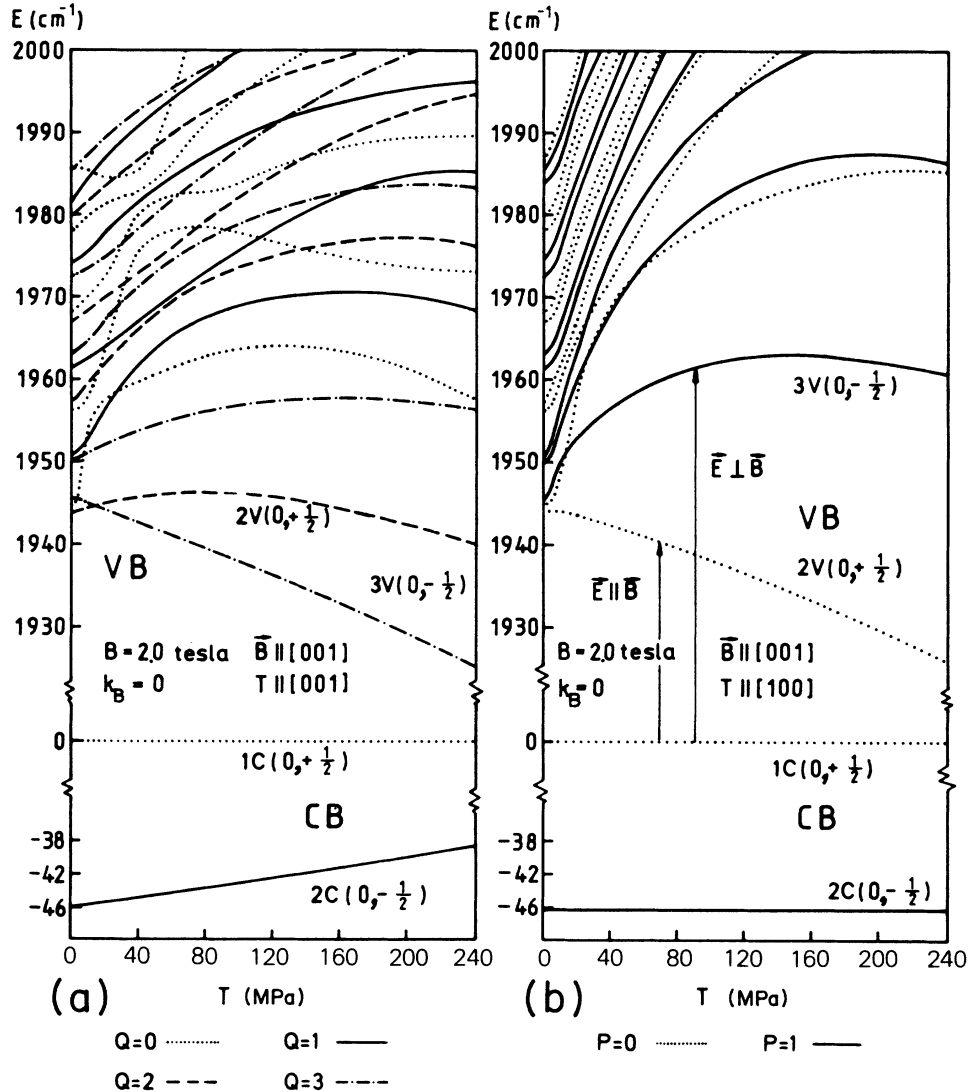
FIG. 2. Stress dependence of the magnetic states for $k_B = 0$ and $B = 2.0$ T parallel to [001] with inverted energy scale. The energies are referred to the lowest conduction state. (a) Parallel stress T along [001]. (b) Transversal stress T along [100].

k-linear terms, the levels avoid crossing in InSb. No trace of this structure has remained in the other geometry [Fig. 2(b)]. Furthermore, when moving from $T\|B$ to $T\bot B$ the valence levels $2V = (0,\frac{1}{2})$ and $3V = (0,-\frac{1}{2})$ interchange and strongly split up with increasing stress.

In the conduction band, for $T\|B$ the g factor decreases linearly with stress. For $T\bot B$ the two spin-split oscillator ground states $1C = (0,\frac{1}{2})$ and $2C = (0,-\frac{1}{2})$ run parallel and document a stress-independent g factor.

VI. INTERBAND TRANSITIONS

In the following, we primarily discuss the geometry $T\bot B\|[001]$. Electrons, which recombine from the lowest conduction level, emit a significant pair of spectral lines [Fig. 2(b)], namely $1C = (0,\frac{1}{2}) \rightarrow 2V = (0,\frac{1}{2})$ and $1C = (0,\frac{1}{2}) \rightarrow 3V = (0,-\frac{1}{2})$. The frequency of the first line

decreases monotonically with stress, the frequency of the second line first increases and then falls away. Line $1C \rightarrow 2V$ is π polarized, because $\Delta P = 0$, and line $1C \rightarrow 3V$ is σ polarized, because $\Delta P = 1$.

The energy separation of the two spin-split conduction states $1C$ and $2C$ does not change with stress. Therefore the stress dependence for recombination radiation, which is emitted from level $2C$, is the same as for radiation from level $1C$. The only difference is a shift by about 46 cm^{-1} and an inverted polarization characteristic (π instead of σ and vice versa). One expects to observe two series of lines which are exact copies, each resembling the behavior of the valence-band structure under stress. Inter- and intraband features are thus seen simultaneously.

For zero stress and $k_B = 0$ the symmetry group of the Hamiltonian is S_4 in both geometries. Dipole radiation accepts S_4 symmetry as equivalent to cylinder symmetry, and σ-polarized light will not display any dependence of
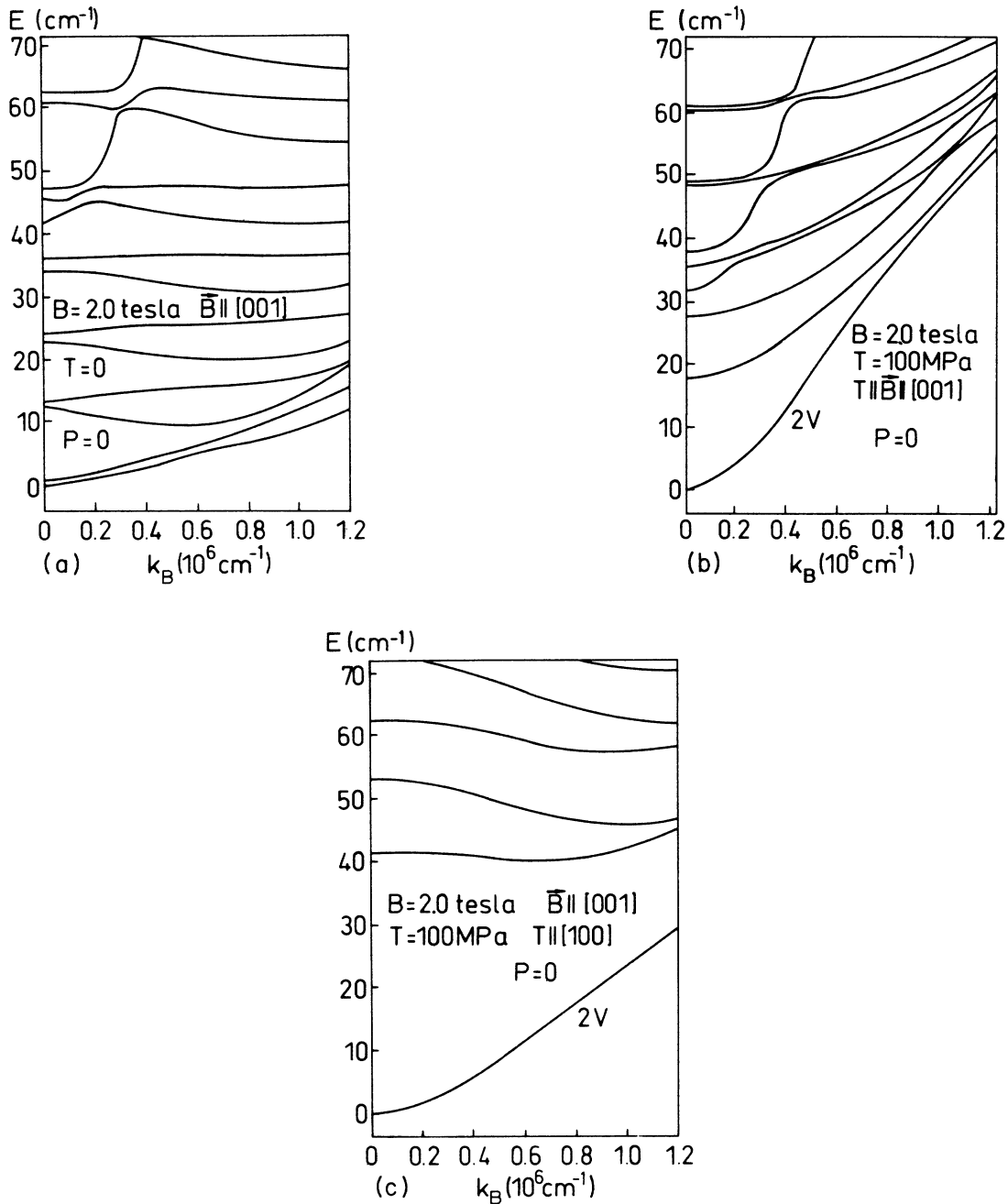
FIG. 3. k_B dependence of the uppermost valence states. Only the representation $P=0$ is drawn. The magnetic field is $B=2.0$ T along [001]. (a) Zero stress. (b) Parallel stress $T=100$ MPa along [001]. (c) Transversal stress $T=100$ MPa along [100].

the angle of the polarization direction in the Voigt configuration (k⊥B, E⊥B). When transversal stress is applied, lowering the symmetry to C_2, an angular dependence of the intensity will be seen, reflecting the twofold symmetry.

VII. k_B DEPENDENCE OF THE VALENCE ENERGIES

The k_B dependence of the magnetic valence states is distinctively different in the two geometries. At zero

stress [Fig. 3(a)] anticrossing effects of neighboring bands cause several noncentral extrema (for clarity only the $P=0$ levels are drawn). However, when stress is applied parallel to the magnetic field, the extrema are straightened, and the bands assume an almost parabolic shape. This is the reason why, in the work of Ranvaud et al.,[10] the valence intraband transitions could be interpreted as central transitions.

Under crossed fields, only the two lowest valence states depend in a parabolic way on k_B, the higher states preserve the off-center extrema. This behavior causes the unusual effects in hole Raman scattering experiments (see

the fourth paper in this series[15]).

For interband transitions, the noncentral maxima are not significant. Due to the strong parabolicity of the conduction states the k_B dependence of the energy separation $\Delta E(k_B)$ always is minimal at $k_B = 0$.

VIII. SUMMARY

In this paper, previous calculations of Landau states in zinc-blende-type crystals, which are exposed to uniaxial stress parallel to the magnetic field, have been extended to a geometry of crossed fields. We established an effective-mass Hamiltonian and diagonalized it with material parameters for InSb. The stress dependence of the states is completely different in the two geometries and gives rise to the expectation that the structure of the valence bands can be illuminated by intra- as well as interband transitions. Experiment justifies this optimism in the following three papers.

*Present address: Telefunken Electronic, D-7100 Heilbronn, West Germany

[1]U. Rössler, Solid State Commun. 49, 943 (1984).

[2]E. O. Kane, J. Phys. Chem. Solids 1, 249 (1957).

[3]P. G. Seiler, B. D. Bajaj, and A. E. Stephens, Phys. Rev. B 16, 2822 (1977).

[4]M. Cardona, N. E. Christensen, and G. Fasol, Phys. Rev. Lett. 56, 2831 (1986).

[5]H. Riechert, S. F. Alvarado, A. N. Titkov, and V. I. Safarov, Phys. Rev. Lett. 52, 2297 (1984).

[6]U. Nowak, E. Gerlach, and W. Richter, Verh. Dtsch. Phys. Ges. 18, 558 (1983).

[7]Y.-F. Chen, M. Dobrowolska, and J. K. Furdyna, Phys. Rev. B 31, 7989 (1985).

[8]M. H. Weiler, R. L. Aggarwal, and B. Lax, Phys. Rev. B 17, 3269 (1978).

[9]K. Suzuki and J. C. Hensel, Phys. Rev. B 9, 4184 (1974); J. C. Hensel and K. Suzuki, Phys. Rev. B 9, 4219 (1974).

[10]The concluding report is given by R. Ranvaud, H.-R. Trebin, U. Rössler, and Fred H. Pollak, Phys. Rev. B 20, 701 (1979).

[11]H.-R. Trebin, U. Rössler, and R. Ranvaud, Phys. Rev. B 20, 686 (1979).

[12]C. L. Littler, D. G. Seiler, R. Kaplan, and R. J. Wagner, Phys. Rev. B 27, 7473 (1983).

[13]B. Wolfstädter, H.-R. Trebin, H. Pascher, and H. G. Häfele, following paper, Phys. Rev. B 37, 10256 (1988) (paper II).

[14]B. Wolfstädter, H.-R. Trebin, H. Pascher, and H. G. Häfele, this issue, Phys. Rev. B 37, 10260 (1988) (paper III).

[15]B. Wolfstädter, H.-R. Trebin, H. Pascher, and H. G. Häfele, this issue, Phys. Rev. B 37, 10264 (1988) (paper IV).

[16]G. L. Bir and G. E. Pikus, Symmetry and Strain-Induced Effects in Semiconductors (Wiley, New York, 1974), Secs. 25 and 26.

[17]N. R. Ogg, Proc. Phys. Soc. London 89, 431 (1966).

[18]C. Hermann and C. Weisbuch, Phys. Rev. B 15, 823 (1977).

[19]M. Cardona, Phys. Rev. B 34, 7402 (1986).